Journal of Waste Management and Reprocessing
Volume 4 | Issue 1
ISSN: 2455-7633

Research Article Open Access

Research on the absorption treatment technology of simulated liquid waste containing tritium for measurement

Wang Yu, Wang Biao, Du Zhi-hui* and Gong Jun-jun

Naval University of Engineering, Wuhan 430033, China

Corresponding author: Zhi-hui, Naval University of Engineering, Wuhan 430033, China,
Email: 3072004003@163.COM

Citation: Wang Yu, Wang Biao, Du Zhi-hui, Gong Jun-jun (2026 Research on the absorption treatment technology of simulated liquid waste containing tritium for measurement. J Waste Manage Repr 4(1) :101

Received Date: July 26, 2026 **Accepted Date:** July 31, 2026 **Published Date:** August 13, 2026

Abstract

To address the safety risks associated with long-term storage of tritium containing measurement waste liquid, this study employed commercial absorbents N910 and N960 for its absorption treatment, and systematically investigated the effects of liquid to solid ratio, temperature, and absorption time on the absorption performance. The results indicated that the optimal liquid to solid ratio for N910 absorbing scintillation cocktail was 1.5:1, and for N960 absorbing water and ethylene glycol, both were 2:1. Under room temperature conditions, all systems achieved relatively high absorption capacities. The absorption equilibrium times for N910 absorbing scintillation cocktail, and N960 absorbing water and ethylene glycol, were all approximately 20 min, with equilibrium absorption capacities of 1.48, 1.99, and 2.00 $g \cdot g^{-1}$, respectively. The pseudo second order kinetic model could well describe the above absorption processes, indicating that all absorption processes were dominated by chemisorption. Based on the optimal liquid to solid ratios for each component, the suitable mixing mass ratio of N960 to N910 was determined to be 5.25:1, and the optimal liquid to solid ratio for the mixed absorbent treating simulated tritium containing measurement waste liquid was 1.5:1, at which the waste liquid could be completely absorbed. This study provides a feasible technical solution for the safe and efficient treatment of tritium containing measurement waste liquid.

Keywords: radioactive organic waste liquid; tritium containing measurement waste liquid; absorption treatment

1. Introduction

The operation, maintenance, and decommissioning of nuclear facilities, as well as environmental monitoring, radioactive experiments, and the utilization of nuclear technology, all generate a certain amount of radioactive organic waste liquid [1-4]. Compared with radioactive wastewater, its generation volume is usually relatively small. However, due to the long-term lack of economical, efficient, and safe treatment technologies, this type of waste liquid is mostly managed through temporary storage in practice, leading to a continuous increase in cumulative storage capacity, which has become one of the important bottlenecks constraining waste minimization and environmental safety in the nuclear industry. More critically, radioactive organic waste liquids generally possess flammability and high volatility, and during long-term storage, there exist safety risks such as leakage and explosion [5-7]. Therefore, the development of reliable treatment technologies suitable for radioactive organic waste liquids is of urgent engineering demand and practical safety significance.

For the treatment of radioactive organic waste liquids, the methods currently reported domestically and internationally mainly include incineration [8, 9], wet oxidation [10, 11], cement solidification [12, 13], and absorption methods [14]. Among them, although incineration and wet oxidation can achieve relatively high volume reduction ratios, they both require the construction of dedicated treatment facilities, and the equipment is prone to severe corrosion under high-temperature or strong oxidizing environments, resulting in high operation and maintenance costs. Cement solidification, though relatively simple in operation, faces challenges such as hydration inhibition, poor compatibility, and unsatisfactory leaching performance when treating complex organic waste liquids. In contrast, the absorption method, with its advantages of simple process flow, stable physicochemical properties of the absorbed solidified forms, and convenience for subsequent transportation and disposal, is generally considered one of the more economical and effective technical routes for the treatment of radioactive organic waste liquids [15, 16].

Tritium-containing measurement waste liquid is a typical and representative special component of radioactive organic waste liquids, mainly derived from the waste liquid generated during the determination of 3H concentration by liquid scintillation counting (LSC). Its basic composition includes scintillation cocktail, ethylene glycol, and a small amount of residual water. This type of waste liquid possesses both the radioactive and organic solvent hazard characteristics, and the risks associated with long-term storage are particularly prominent. To this end, based on a systematic investigation of the properties of existing absorbent materials, this study intends to select two absorbents, N910 and N960, which exhibit excellent engineering performance, to systematically investigate the effects of key process parameters such as liquid-to-solid ratio, temperature, and absorption time on the absorption efficiency and the quality of the solidified form, taking into account the actual material characteristics of tritium-containing measurement waste liquid. The aim is to provide experimental basis and theoretical guidance for the safe treatment of tritium-containing measurement waste liquid.

2. Materials and Methods

2.1 Main Experimental Materials and Equipment

The main reagents used in this study and their sources are as follows: two commercial absorbents, N910 and N960, were purchased from Nochar Inc. (USA); the scintillation cocktail (ULTIMAGOLD, Cat. No. 6013326) was purchased from PerkinElmer Inc. (USA); ethylene glycol (analytical grade) was purchased from Xilong Chemical Co., Ltd. (China). Deionized water with a conductivity of less than 5 μS⊠cm-1 was used throughout the experiments.

The main experimental equipment included: a precision electronic balance (Model AL204, Mettler Toledo Instruments (Shanghai) Co., Ltd., China); a benchtop high speed centrifuge (Model H/T16MM, Hunan Hexi Instrument Equipment Co., Ltd., China); and an electric blast drying oven (Model DHG 9025A, Shanghai Boxin Instrument Equipment Factory, China).

2.2 Material Characterization Methods

(1) Scanning Electron Microscopy (SEM)

The surface morphologies of N910 and N960 were observed using a TESCAN MIRA3 scanning electron microscope (TESCAN, Czech Republic) at an accelerating voltage of 5 kV.

(2) Fourier Transform Infrared Spectroscopy (FT-IR)

Infrared spectra of N910 and N960 were recorded on a Nicolet iS50 Fourier transform infrared spectrometer (Thermo Fisher Scientific, USA). The samples were prepared using the KBr pellet method, and the spectra were collected in the wavenumber range of 400–4000 cm^{-1} with a resolution of 0.5 cm^{-1}.

(3) Thermogravimetry-Differential Scanning Calorimetry (TG-DSC)

The thermal decomposition behavior and thermal effects of N910 and N960 were analyzed using a Netzsch STA 449F3 synchronous thermal analyzer (NETZSCH, Germany). The measurements were carried out under a high-purity argon atmosphere, with the temperature program set to rise from room temperature to 800 °C at a heating rate of 10 °C.min^{-1}.

2.3 Experimental Methods for Absorption Performance

To systematically evaluate the absorption performance of the two absorbents (N910 and N960) toward tritium-containing measurement waste liquid and its components, this study investigated the effects of liquid-to-solid ratio, temperature, and absorption time on the absorption performance, and on this basis, conducted absorption kinetic analysis and absorption experiments of the mixed absorbent for simulated tritium-containing measurement waste liquid. All absorption experiments were carried out in glass tubes with filter screens, and the centrifugation conditions were uniformly set at a rotational speed of 2,500 r.min^{-1} for 2 min.

(1) Effect of liquid-to-solid ratio on absorption performance

Under room temperature conditions, 2.0 g of absorbent (N910 or N960) was accurately weighed and placed into a glass tube with a filter screen, and different masses of the absorption object were added. After absorption for 30 min, the glass tube was placed in a centrifuge for solid-liquid separation, and the absorption capacity (q) and unabsorbed amount (q') were calculated according to the following equations

The absorption capacity was calculated as

$$q = \frac{m_1 - m}{m} \quad (1)$$

where q is the absorption capacity ($g.g^{-1}$); m is the mass of the absorbent before absorption (g); and m1 is the mass of the absorbent after absorption (g).

The unabsorbed amount was calculated as:

$$q' = \frac{m_2 - (m_1 - m)}{m} \quad (2)$$

where q′ is the unabsorbed amount ($g.g^{-1}$); and m2 is the mass of the absorption object added (g).

(2) Effect of temperature on absorption performance

2.0 g of absorbent was accurately weighed and placed into a glass tube with a filter screen, and the absorption object was added at a fixed liquid-to-solid ratio. Absorption was conducted at constant temperatures of 25 °C, 30 °C, 40 °C, 50 °C, and 60 °C for 30 min. After absorption, solid-liquid separation was performed under the above centrifugation conditions, and the absorption capacity was determined by weighing.

(3) Effect of time on absorption performance

Under room temperature conditions, 2.0 g of absorbent was accurately weighed and placed into a glass tube with a filter screen, and the absorption object was added at a fixed liquid-to-solid ratio. After absorption for 1, 5, 10, 20, and 30 min, respectively, solid-liquid separation was performed under the above centrifugation conditions, and the absorption capacity at each time point was determined by weighing.

(4) Absorption kinetic analysis

To gain a deeper understanding of the absorption behavior and rate-controlling mechanism of the absorbents, the pseudo-second-order kinetic model was employed to fit the kinetic processes of N910 absorbing scintillation cocktail, and N960 absorbing water and ethylene glycol. The linear form of the pseudo-second-order kinetic equation is as follows [17]:

$$\frac{t}{q_t} = \frac{1}{k_2 q_e^2} + \frac{t}{q_e} \quad (3)$$

where qe is the equilibrium absorption capacity ($g.g^{-1);}$ qt is the absorption capacity at time t ($g.g^{-1}$); and k_2 is the pseudo-second-order rate constant ($g.g^{-1}.min^{-1}$).

(5) Absorption performance of the mixed absorbent of N910 and N960 for simulated tritium-containing measurement waste liquid

The simulated tritium-containing measurement waste liquid was prepared by mixing ethylene glycol, scintillation cocktail, and deionized water at a volume ratio of 6:1:1. According to the physicochemical properties of the components, ethylene glycol and water are polar solvents and are preferably absorbed by hydrophilic absorbents, while the scintillation cocktail is a hydrophobic organic phase and is preferably absorbed by lipophilic absorbents. Therefore, in this study, the lipophilic absorbent N910 and the hydrophilic absorbent N960 were mixed at a certain ratio to achieve synergistic absorption of the multi-components in the simulated waste liquid.

Under room temperature conditions, 2.0 g of the mixed absorbent (total mass of N910 and N960) was accurately weighed and placed into a glass tube with a filter screen, and different volumes of the simulated tritium-containing measurement waste liquid were added. After absorption for 30 min, solid-liquid separation was performed under the above centrifugation conditions, and the absorption capacity and unabsorbed amount were determined by weighing.

3 Results and Analysis

3.1 Characterization of Materials

(1) SEM analysis

(Figure 1 and Figure 2) present the SEM images of N910 and N960 at different magnifications, respectively.

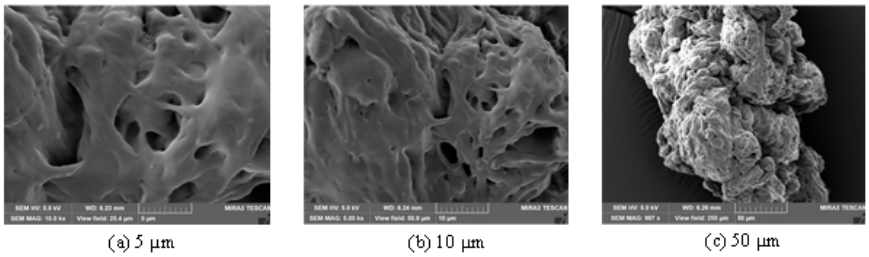

Figure 1. SEM images of N910 on different scales

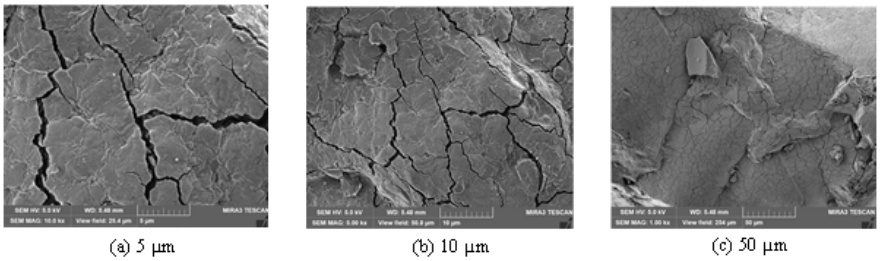

Figure 2. SEM images of N960 on different scales

As shown in Fig. 1, N910 exhibits a typical porous network skeleton structure with abundant pore structures. This three-dimensional interconnected porous configuration facilitates the rapid entry of absorption objects (liquid organic compounds and water) into the absorbent interior through capillary effects, thereby promoting the mass transfer efficiency of the absorption process [18, 19]. In contrast, Fig. 2 reveals that the surface of N960 is relatively dense and smooth, with an overall porosity significantly lower than that of N910. However, several micro cracks and irregular folds can be observed on its surface. These cracks may originate from shrinkage stresses during material preparation [20] and can serve as initial intrusion channels for liquid molecules during the absorption process, contributing to an enhanced absorption rate. In summary, both the well-developed pores of N910 and the surface crack structures of N960 provide favorable physical foundations for the absorption process.

(2) FT-IR analysis

(Figure 3) Shows the Fourier transform infrared spectra of N910 and N960 in the range of 400–4000 cm^{-1}.

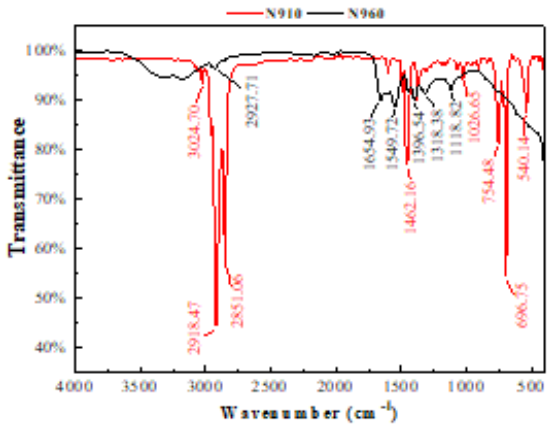

Fig. 3 FT-IR spectrum of N910 and N960

Figure 3. FT-IR spectrum of N910 and N960

As can be seen from (Figure 3), for N910, eight major absorption peaks are present in the spectrum. Among them, the absorption bands at 2918 cm^{-1} and 2851 cm^{-1} can be assigned to the asymmetric and symmetric stretching vibrations of saturated

alkane C–H bonds, indicating the presence of methylene structural units in the molecular chain. The absorption bands at 1462 cm^{-1} and 754 cm^{-1} correspond to the C=C stretching vibration of the benzene ring skeleton and the out-of-plane bending vibration of benzene ring substituents, respectively, suggesting the possible existence of ortho-disubstituted or mono-substituted benzene structures. The absorption band at 1027 cm^{-1} can be attributed to the in-plane bending vibration of C–H in alkenes or the in-plane deformation vibration of C–H on the benzene ring. The absorption band at 697 cm-1 further confirms the presence of mono-substituted benzene rings. Based on the above peak assignments, the molecular structure of N910 contains independent benzene ring units connected by hydrocarbon chains, exhibiting typical aromatic polymer characteristics.

For N960, six major absorption peaks are observed in the spectrum. The absorption band at 2928 cm-1 is attributed to the C–H stretching vibration of alkanes. The absorption band at 1655 cm-1 can be assigned to the amide I band (C=O stretching vibration) or the C=C stretching vibration of aromatic rings. The absorption band at 1550 cm-1 can be attributed to the amide II band (coupled N–H bending and C–N stretching vibrations) or the characteristic absorption of aromatic amines/imines. The absorption band at 1119 cm-1 can be assigned to the asymmetric stretching vibration of C–O–C (aryl ethers) or the C–N stretching vibration of aliphatic amines. A comprehensive analysis indicates that the chemical structure of N960 likely belongs to aromatic/aliphatic polymer materials containing amide or amine groups, with polar functional group characteristics, which provides a molecular-level explanation for its hydrophilic absorption behavior.

(3) TG-DSC analysis

(Figure 4 and Figure 5) present the TG-DSC synchronous thermal analysis curves of N910 and N960, respectively, measured under an argon atmosphere at a heating rate of 10 °C.min-1.

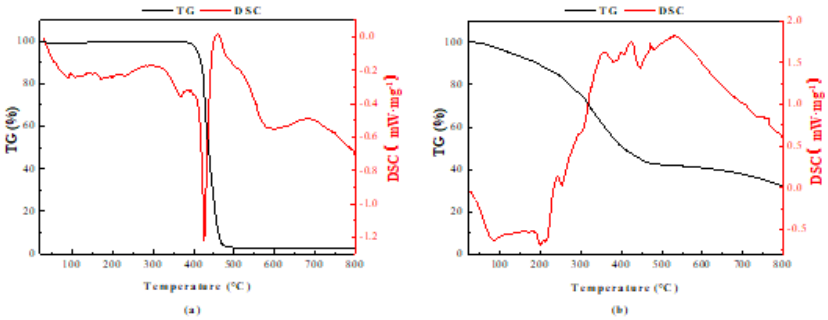

Figure 4. TG-DSC spectrum of N910 (a) and N960 (b)

As shown in (Figure 4a), N910 exhibits no significant mass loss in the range from room temperature to 420 °C, indicating excellent thermal stability within this temperature range. When the temperature rises to 420.1 °C, an obvious exothermic peak appears on the DSC curve, accompanied by a sharp decrease in the TG curve, indicating that N910 undergoes a drastic thermal decomposition reaction at this temperature. The mass loss mainly occurs between 420.1 °C and 450 °C, after which the TG curve levels off, and the final residual mass is approximately 2.9% of the initial mass, which is presumed to be amorphous carbon or carbonized products formed during thermal decomposition.

As shown in (Figure 4b), the thermal decomposition behavior of N960 is significantly different from that of N910. A slow continuous mass loss begins near 60 °C, and the cumulative mass loss reaches approximately 83.3% at about 253 °C; this stage is attributed to the desorption of moisture adsorbed from the environment and the volatilization of residual solvents. After 253 °C, the mass loss rate accelerates markedly, due to the thermal cracking reaction of the polymer main chain. After 408 °C, the mass loss rate slows down again, and the final residual mass is approximately 49.6% of the initial mass. It should be noted that the TG curve of N960 does not exhibit a steep mass-loss step as seen for N910, indicating that its thermal decomposition is a multi-step and relatively mild process, which may involve the progressive detachment of side groups accompanied by main-chain

scission. This thermal behavior characteristic is related to the thermal instability of polar side groups (such as amide or amine groups) present in the molecular structure of N960, which can undergo elimination or cleavage reactions at relatively lower temperatures [21-23].

3.2 Absorption Performance of N910 for Scintillation Cocktail

(1) Effect of liquid-to-solid ratio on the absorption performance of N910 for scintillation cocktail

(Figure 5) presents the variation of absorption capacity and unabsorbed amount of N910 for scintillation cocktail with liquid--to-solid ratio increasing from 1:1 to 4:1 under room temperature conditions.

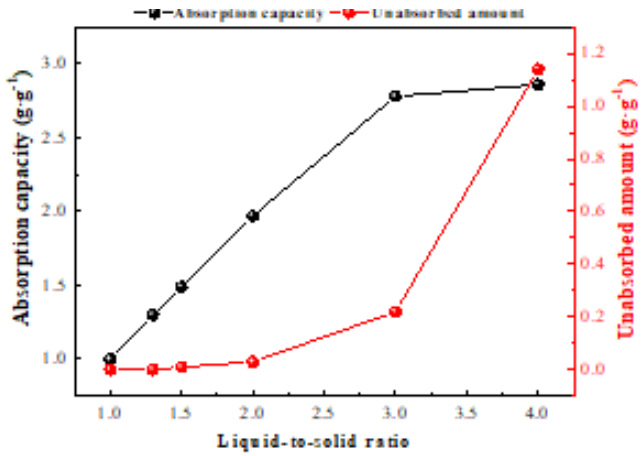

Figure 5. Effect of liquid/solid ratio on absorption of scintillation cocktail by N910

As shown in (Figure 5), with increasing liquid-to-solid ratio, the absorption capacity of N910 for scintillation cocktail exhibits a trend of rapid initial increase followed by leveling off. When the liquid-to-solid ratio increases from 1:1 to 1.5:1, the absorption capacity increases significantly, indicating that the effective adsorption sites on the absorbent surface have not yet been fully occupied, allowing liquid molecules to fully enter the internal pores of the absorbent. When the liquid-to-solid ratio exceeds 1.5:1, the increase in absorption capacity slows down and gradually reaches saturation at a liquid-to-solid ratio of 3:1, suggesting that the absorption capacity of the absorbent approaches its limit. Meanwhile, the unabsorbed amount shows a two-stage variation with increasing liquid-to-solid ratio: when the liquid-to-solid ratio is below 1.5:1, the increase in unabsorbed amount is relatively small; however, when the liquid-to-solid ratio exceeds 1.5:1, the unabsorbed amount increases sharply, indicating that excessive scintillation cocktail has exceeded the treatment capacity of the absorbent, and a large amount of free liquid begins to appear in the system. Considering both absorption efficiency and economic viability, the optimal liquid-to-solid ratio was determined to be 1.5:1. This ratio ensures complete absorption of the scintillation cocktail while maximizing the utilization efficiency of the absorbent.

(2) Effect of temperature on the absorption performance of N910 for scintillation cocktail

Under the condition of a fixed liquid-to-solid ratio of 1.5:1, the effect of temperature on the absorption performance of N910 for scintillation cocktail was investigated in the range of 25 °C to 60 °C, and the results are shown in (Figure 6)

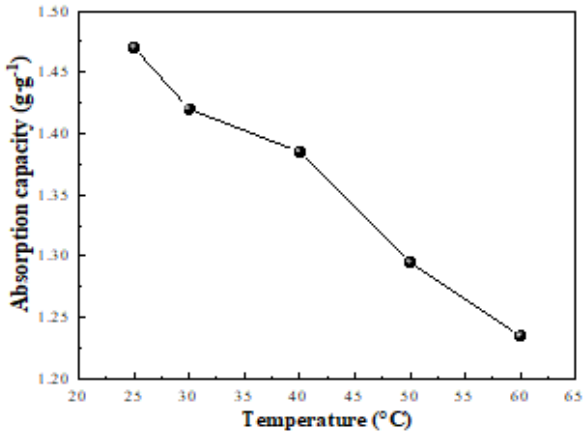

Figure 6. Effect of temperature on absorption of scintillation cocktail by N910

As can be seen from Fig. 6, temperature has a significant effect on the absorption performance of N910. As the temperature increases from 25 °C to 60 °C, the absorption capacity shows a continuous decreasing trend. This phenomenon can be explained from the following two aspects: on the one hand, the absorption process of N910 for scintillation cocktail is dominated by physical adsorption or chemisorption, and increasing temperature may weaken the interaction forces (such as van der Waals forces and hydrogen bonding) between the absorbent and scintillation cocktail molecules, thereby reducing the absorption capacity; on the other hand, the increase in temperature leads to a decrease in the viscosity of the scintillation cocktail and an intensification of molecular thermal motion, which, although favorable for the diffusion of liquid toward the absorbent surface, may also accelerate the desorption rate of already adsorbed molecules, thus reducing the net absorption capacity [24, 25]. From the perspective of engineering application, the storage and treatment of tritium-containing measurement waste liquid are typically conducted under room temperature conditions, and the absorption performance near 25 °C is already sufficient to meet practical requirements.

(3) Effect of absorption time on the absorption performance of N910 for scintillation cocktail

Under the conditions of a liquid-to-solid ratio of 1.5:1 and room temperature, the effect of absorption time on the absorption performance of N910 for scintillation cocktail was investigated, and the results are shown in (Figure 7).

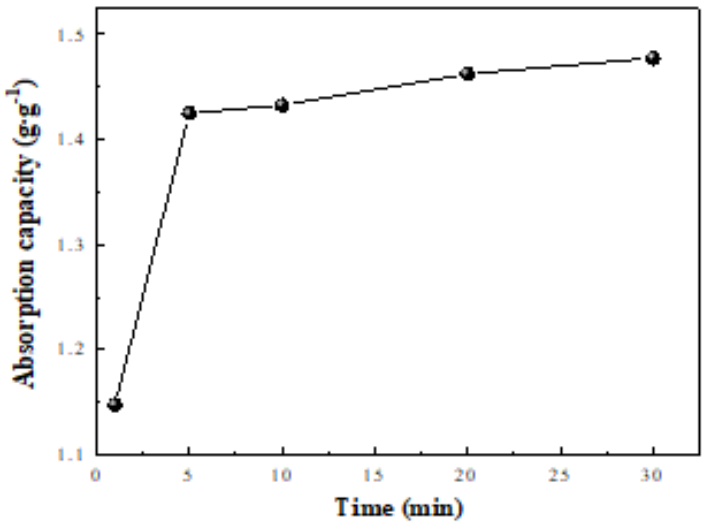

Figure 7. Effect of absorption time on absorption of scintillation cocktail by N910

As shown in (Figure 7), the absorption process of N910 for scintillation cocktail exhibits typical characteristics of a rapid initial

absorption stage followed by a slow equilibrium stage. In the initial stage of absorption (0–5 min), the absorption capacity increases approximately linearly with time, because at this time the absorbent surface possesses a large number of unoccupied active sites, and the concentration gradient of the scintillation cocktail is relatively large, providing a strong mass transfer driving force. As absorption proceeds, the surface active sites are gradually occupied, and liquid molecules need to diffuse into the deeper internal pores of the absorbent, resulting in increased mass transfer resistance and a gradual decrease in the absorption rate. After approximately 20 min, the absorption capacity essentially stabilizes and reaches the absorption equilibrium state, with an equilibrium absorption capacity of approximately 1.48 $g.g^{-1}$. This result indicates that N910 exhibits a fast absorption rate and high absorption capacity for scintillation cocktail, which is favorable for rapid treatment requirements in practical engineering applications.

(4) Absorption kinetics of N910 for scintillation cocktail

To further explore the absorption mechanism and rate-controlling steps of N910 for scintillation cocktail, the pseudo-second-order kinetic model was employed to fit the experimental data. The absorption capacity data at different time points were linearly regressed by plotting t/qt against t, and the fitting results are shown in (Figure 8).

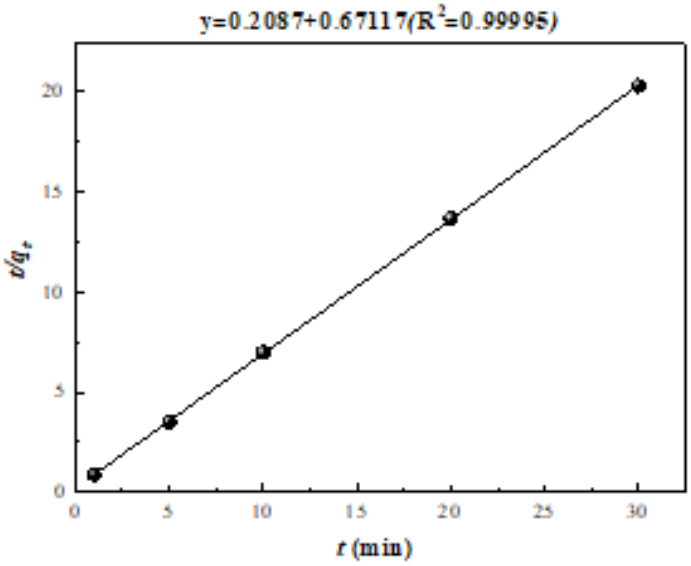

Figure 8. Pseudo-second-order kinetic plot for scintillation cocktail absorption on N910

As shown in (Figure 8), the pseudo-second-order kinetic model exhibits a good fitting effect on the experimental data, with the linear correlation coefficient R2 approaching unity. The theoretical equilibrium absorption capacity calculated from the slope of the fitted straight line is 1.49 $g.g^{-1}$, which is in excellent agreement with the experimentally measured equilibrium absorption capacity (1.48 $g.g^{-1}$), with a relative deviation of less than 1%. This result indicates that the pseudo-second-order kinetic model can well describe the entire absorption process of N910 for scintillation cocktail, suggesting that the absorption process of N910 for scintillation cocktail is dominated by chemisorption. This mechanistic interpretation is consistent with the characteristics of the N910 molecular structure containing aromatic rings and polar functional groups, where the organic molecules in the scintillation cocktail may form π-π stacking interactions or hydrophobic interactions with these functional groups, thereby achieving efficient absorption.

3.3 Absorption Performance of N960 for Water

(1) Effect of liquid-to-solid ratio on the absorption performance of N960 for water

(Figure 9) presents the variation of absorption capacity and unabsorbed amount of N960 for water with liquid-to-solid ratio increasing from 1:1 to 4:1 under room temperature conditions.

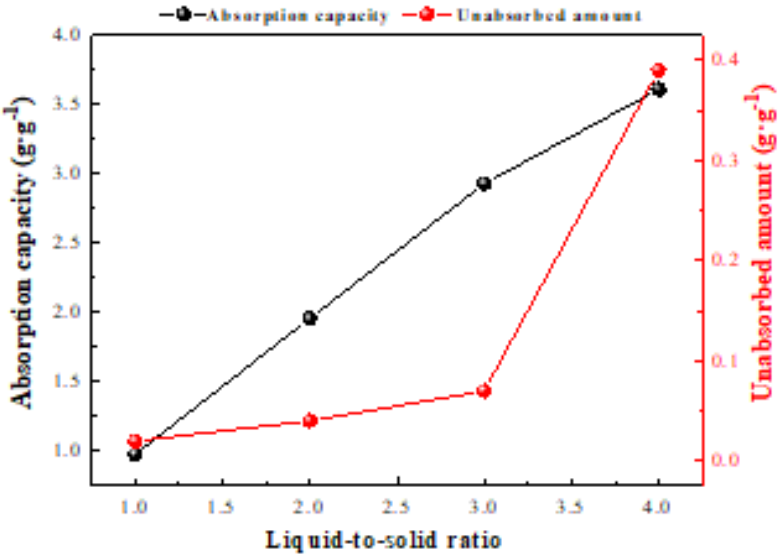

Figure 9. Effect of liquid/solid ratio on absorption of water by N960

As shown in (Figure 9), the absorption capacity of N960 for water exhibits a continuous increasing trend with increasing liquid-to-solid ratio, and the unabsorbed amount also increases simultaneously. This phenomenon indicates that within the investigated liquid-to-solid ratio range, the absorption capacity of N960 has not yet reached complete saturation. However, when the liquid-to-solid ratio exceeds 2:1, the increase in unabsorbed amount becomes significantly larger, indicating that a large amount of free water remains unabsorbed in the system. From the perspective of practical engineering application, an excessively high liquid-to-solid ratio not only causes waste of the absorbent but also leaves a large amount of free liquid in the system after absorption, which is unfavorable for subsequent solidification treatment and disposal. Considering both absorption efficiency and material economy, the optimal liquid-to-solid ratio was determined to be 2:1.

(2) Effect of temperature on the absorption performance of N960 for water

Under the condition of a fixed liquid-to-solid ratio of 2:1, the effect of temperature on the absorption performance of N960 for water was investigated, and the results are shown in (Figure 10).

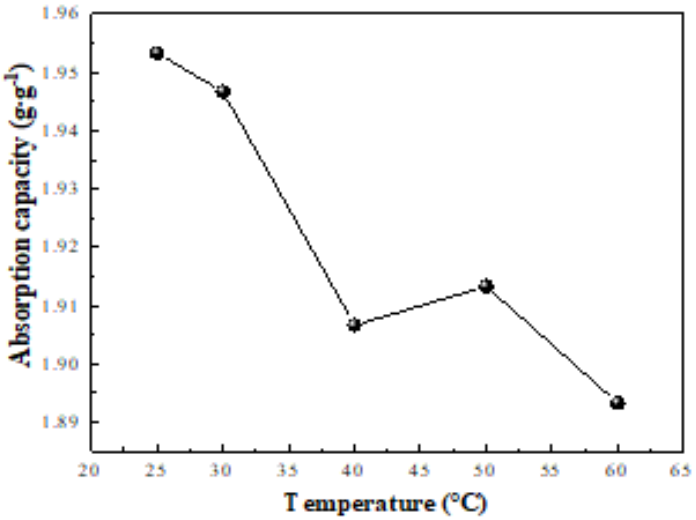

Figure 10. Effect of temperature on absorption of water by N960

As can be seen from Fig. 10, the absorption capacity of N960 for water shows a continuous decreasing trend with increasing temperature. This temperature dependence can be explained by the thermodynamic nature of the absorption process. The molecular structure of N960 is rich in polar functional groups such as amide groups and amine groups, and its combination with water molecules is mainly achieved through hydrogen bonding. The formation of hydrogen bonds is typically an exothermic process, and increasing temperature is unfavorable for the formation and stability of hydrogen bonds, causing the already bound water molecules to tend to desorb, thereby reducing the equilibrium absorption capacity [26].

(3) Effect of absorption time on the absorption performance of N960 for water

Under the conditions of a liquid-to-solid ratio of 2:1 and room temperature, the effect of absorption time on the absorption performance of N960 for water was investigated, and the results are shown in (Figure 11).

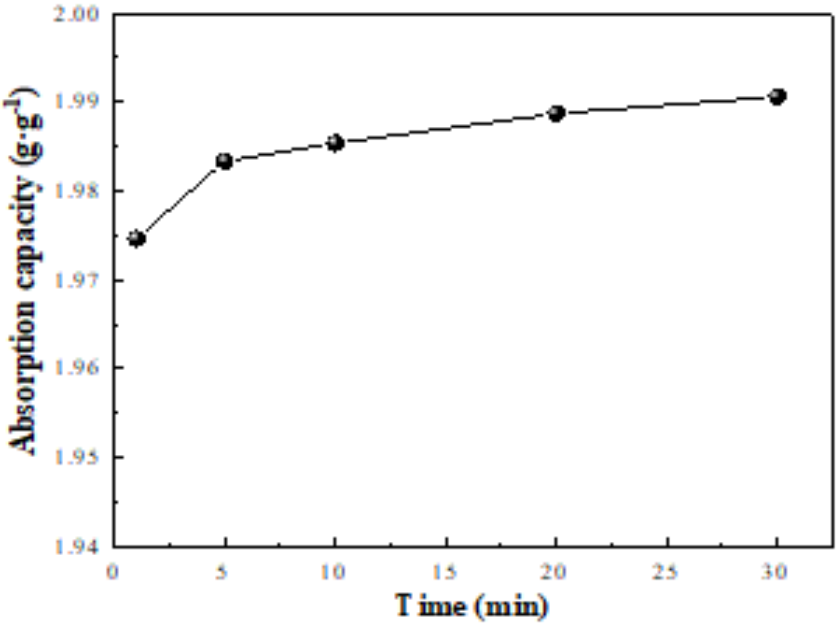

Figure 11. Effect of absorption time on absorption of water by N910

As shown in (Figure 11), the absorption process of N960 for water also exhibits typical characteristics of a rapid initial absorption stage followed by a slow equilibrium stage. In the initial stage of absorption (0–5 min), the absorption capacity increases rapidly with time, attributed to the rapid combination between the abundant polar sites on the absorbent surface and a large number of water molecules, as well as the rapid filling of water molecules into the surface cracks and pores of the absorbent through capillary effects. Subsequently, the absorption rate gradually slows down, entering a slow stage controlled by the diffusion of water molecules into the interior of the absorbent. After approximately 20 min, the absorption capacity stabilizes and reaches the absorption equilibrium state, with an equilibrium absorption capacity of approximately 1.99 $g.g^{-1}$.

(4) Absorption kinetics of N960 for water

To quantitatively describe the absorption rate and mechanism of N960 for water, the pseudo-second-order kinetic model was employed to fit the experimental data. Linear regression was performed by plotting t/qt against t, and the fitting results are shown in (Figure 12).

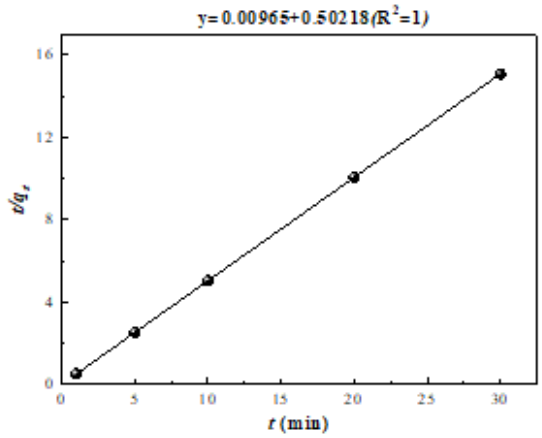

Figure 12. Pseudo-second-order kinetic plot for water absorption on N960

As shown in Fig. 12, the correlation coefficient obtained from the fitting is 1; the equilibrium absorption capacity qe calculated from the slope of the fitted line is 1.99 $g.g^{-1}$, which is consistent with the experimental value (1.99 $g.g^{-1}$). This indicates that the pseudo-second-order kinetic equation can well describe the absorption process of N960 for water, suggesting that the absorption process of N960 for water is dominated by chemisorption. As shown in (Figure 13), the pseudo-second-order kinetic model exhibits an excellent fitting effect for the absorption of water by N960, with the linear correlation coefficient R^2 approaching unity. The theoretical equilibrium absorption capacity calculated from the slope of the fitted line is 1.99 $g.g^{-1}$, which is in complete agreement with the experimental value (1.99 $g.g^{-1}$). This result indicates that the pseudo-second-order kinetic model can well describe the entire absorption process of N960 for water, demonstrating that the absorption process of N960 for water is dominated by chemisorption, and the dominant interaction force remains the hydrogen bonding between the polar sites of amide groups and amine groups on the N960 molecular chain and water molecules.

3.4 Absorption Performance of N960 for Ethylene Glycol

(Figure 13) presents the variation of absorption capacity and unabsorbed amount of N960 for ethylene glycol with liquid-to--solid ratio increasing from 0.5:1 to 3:1 under room temperature conditions.

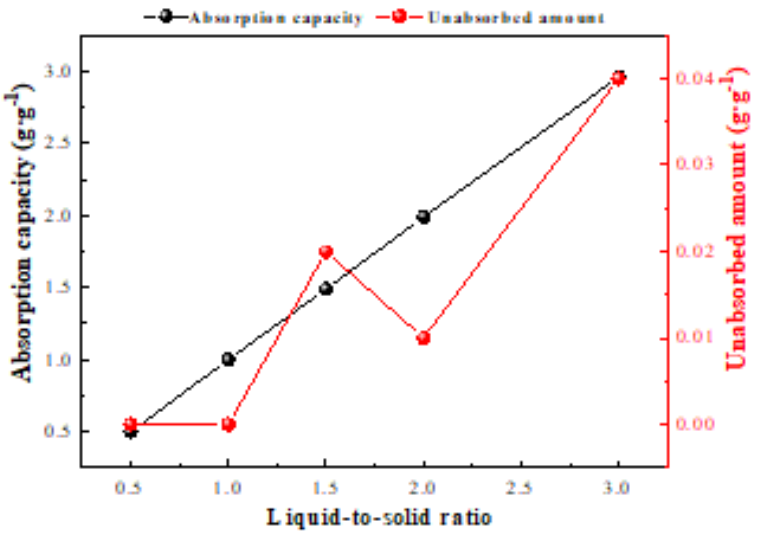

Figure 13. Effect of liquid/solid ratio on absorption of ethylene glycol by N960

As shown in Fig. 13, the absorption capacity of N960 for ethylene glycol exhibits a continuous increasing trend with increasing

liquid-to-solid ratio, and the unabsorbed amount also increases gradually. When the liquid-to-solid ratio increases from 0.5:1 to 2:1, the increase in absorption capacity is relatively significant, indicating that the active sites of the absorbent are gradually occupied by ethylene glycol molecules. When the liquid-to-solid ratio exceeds 2:1, the increase in unabsorbed amount accelerates markedly, and the increasing trend of absorption capacity tends to level off, indicating that the dosage of ethylene glycol has exceeded the carrying capacity of the absorbent, and a large amount of free liquid appears in the system. Considering both absorption efficiency and material economy, the optimal liquid-to-solid ratio was determined to be 2:1. Under this ratio, the absorption capacity of N960 for ethylene glycol is fully utilized, while waste caused by excess absorbent is avoided.

(2) Effect of temperature on the absorption performance of N960 for ethylene glycol

Under the condition of a fixed liquid-to-solid ratio of 2:1, the effect of temperature on the absorption performance of N960 for ethylene glycol was investigated, and the results are shown in (Figure 14).

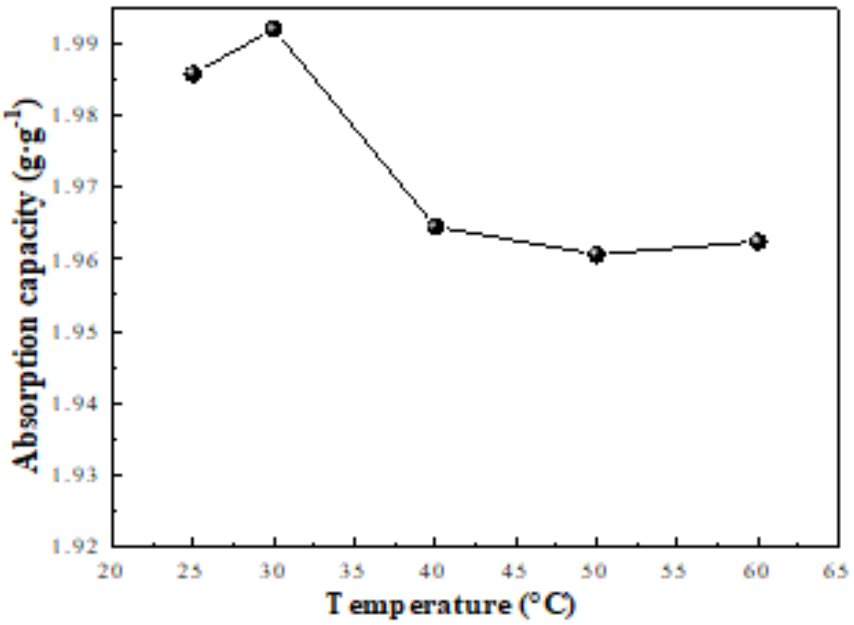

Figure 14. Effect of temperature on absorption of ethylene glycol by N960

As shown in Fig. 14, with increasing temperature, the absorption capacity of N960 for ethylene glycol exhibits a trend of slight initial decrease followed by stabilization. Compared with the absorption behavior of N960 for water, the ethylene glycol system shows significantly lower temperature sensitivity. Throughout the entire experimental temperature range, the absorption capacity remains within the narrow range of 1.96–2.00 $g.g^{-1}$, with a maximum variation of only about 2%. This phenomenon can be explained from the following two aspects: on the one hand, the ethylene glycol molecule contains two hydroxyl groups (-OH) and possesses strong polarity, which enables it to form hydrogen bonding with the amide groups and amine groups on the N960 molecular chain; on the other hand, the molecular size of ethylene glycol is larger and its viscosity is higher, and the rate of its diffusion into the absorbent interior is affected by temperature in a more complex manner. Although increasing temperature is favorable for reducing the system viscosity and promoting molecular diffusion, it also weakens the strength of hydrogen bonding, and the competitive effect of these two factors may result in a relatively small variation of net absorption capacity with temperature [27]. From the perspective of engineering application, N960 exhibits good temperature adaptability for the absorption of ethylene glycol, maintaining stable absorption performance at room temperature and under certain elevated temperature conditions.

(3) Effect of absorption time on the absorption performance of N960 for ethylene glycol

Under the conditions of a liquid-to-solid ratio of 2:1 and room temperature, the effect of absorption time on the absorption performance of N960 for ethylene glycol was investigated, and the results are shown in (Figure 15).

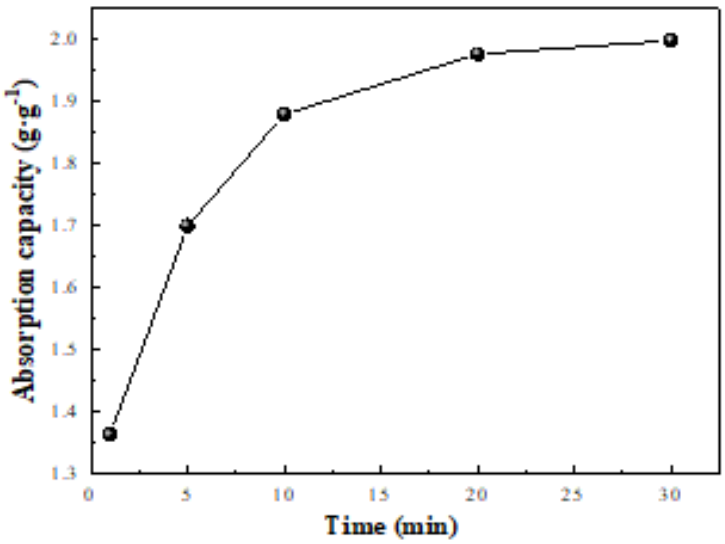

Figure 15. Effect of absorption time on absorption of ethylene glycol by N960

As shown in Fig. 15, the absorption process of N960 for ethylene glycol exhibits similar stage characteristics to the systems described above. In the initial stage of absorption (0–5 min), the absorption capacity increases rapidly with time, attributed to the rapid combination between the abundant polar active sites on the absorbent surface and ethylene glycol molecules. In the subsequent 5–20 min, the absorption rate gradually slows down, mainly controlled by the diffusion of ethylene glycol molecules into the internal pores of the absorbent and their combination with the deeper active sites. After approximately 20 min, the absorption capacity essentially stabilizes and reaches the absorption equilibrium state, with an equilibrium absorption capacity of approximately 2.00 $g.g^{-1}$. It is noteworthy that the equilibrium absorption capacity of N960 for ethylene glycol (2.00 g.g-1) is very close to that for water (1.99 $g.g^{-1}$), both at approximately 2.00 $g.g^{-1}$. This similarity indicates that the absorption capacity of N960 for polar small molecules mainly depends on the density of its polar functional groups (amide/amine groups), rather than the specific type of the absorbate molecules. Although the molecular weight of ethylene glycol is larger than that of water, each of its molecules contains two hydroxyl groups, which can provide two hydrogen bonding sites; therefore, the saturation absorption capacity per unit mass of absorbent is comparable to that for water.

(4) Absorption kinetics of N960 for ethylene glycol

To quantitatively describe the absorption kinetic characteristics of N960 for ethylene glycol, the pseudo-second-order kinetic model was employed to fit the experimental data. Linear regression was performed by plotting t/qt against t, and the fitting results are shown in (Figure 16).

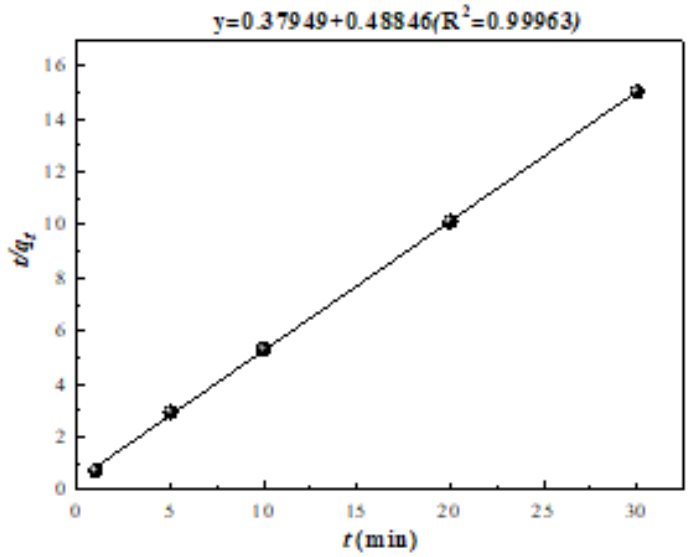

Figure 16. Pseudo-second-order kinetic plot for ethylene glycol absorption on N960

As shown in (Figure 16), the pseudo-second-order kinetic model exhibits an excellent fitting effect for the absorption of ethylene glycol by N960, with the linear correlation coefficient (R^2) approaching unity. The theoretical equilibrium absorption capacity calculated from the slope of the fitted line is 2.05 $g.g^{-1}$, which is basically consistent with the experimental equilibrium absorption capacity (2.00 $g.g^{-1}$), with a relative deviation of approximately 2.5%, within the allowable range of experimental error. This result further verifies that the pseudo-second-order kinetic model can well describe the entire absorption process of N960 for ethylene glycol, indicating that the absorption process of N960 for ethylene glycol is dominated by chemisorption. For the N960-ethylene glycol system, the dominant interaction force is the hydrogen bonding network formed between the polar functional groups (amide groups and amine groups) on the N960 molecular chain and the hydroxyl groups (-OH) of ethylene glycol.

3.5 Absorption Performance of N910 and N960 for Simulated Tritium-Containing Measurement Waste Liquid

The main components of the tritium-containing measurement waste liquid are ethylene glycol, scintillation cocktail, and water, with a volume ratio of approximately 6:1:1. Among them, the scintillation cocktail is a hydrophobic organic phase and is preferably absorbed by the lipophilic absorbent N910; ethylene glycol and water are both polar solvents and are preferably absorbed by the hydrophilic absorbent N960. Therefore, to achieve synergistic absorption of the multi-components in the simulated tritium-containing measurement waste liquid, N910 and N960 need to be mixed at a certain ratio. From Sections 3.2 to 3.4, it can be seen that the optimal liquid-to-solid ratio for N910 absorbing scintillation cocktail is 1.5:1, and the optimal liquid-to-solid ratios for N960 absorbing water and ethylene glycol are both 2:1. Therefore, to effectively absorb the tritium-containing measurement waste liquid, when N960 and N910 are used in combination, the mass ratio should be 5.25:1.

After thoroughly mixing N960 and N910 at a mass ratio of 5.25:1, under room temperature conditions, the absorption performance of the mixed absorbent for the simulated tritium-containing measurement waste liquid was investigated at liquid-to--solid mass ratios of 0.5:1, 0.75:1, 1:1, 1.25:1, 1.5:1, and 2:1, and the results are shown in (Figure 17).

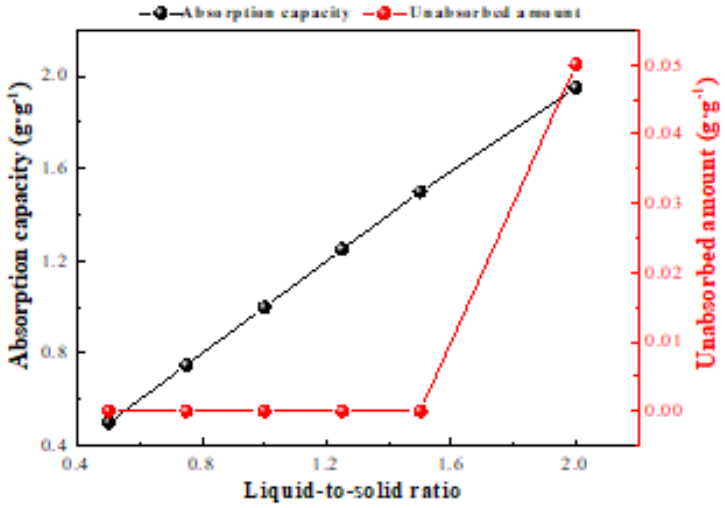

Figure 17. Absorption performance of simulated liquid waste containing tritium for measurement by N910 and N960

As shown in (Figure 17), with increasing liquid-to-solid ratio, the absorption capacity of the mixed absorbent for the simulated tritium-containing measurement waste liquid exhibits a continuous increasing trend. When the liquid-to-solid ratio is below 1.5:1, the simulated waste liquid can be completely absorbed, with almost no free liquid remaining in the system, indicating that the absorption capacity of the mixed absorbent is sufficient to carry the added waste liquid volume. When the liquid-to--solid ratio exceeds 1.5:1, the unabsorbed amount increases significantly, indicating that the excess simulated waste liquid has exceeded the maximum absorption capacity of the mixed absorbent, and a large amount of free liquid begins to appear in the system, which not only reduces the absorption efficiency but also has adverse effects on subsequent solidification treatment and disposal. Based on comprehensive consideration, the optimal liquid-to-solid ratio for the mixed absorbent and the simulated tritium-containing measurement waste liquid was determined to be 1.5:1. Under this ratio, the mixed absorbent can achieve complete absorption of the simulated waste liquid while ensuring relatively full utilization of the absorbent. It is worth noting that the optimal liquid-to-solid ratio of the mixed absorbent (1.5:1) is consistent with that of N910 alone for absorbing scintillation cocktail, but lower than the optimal liquid-to-solid ratios for N960 alone absorbing water or ethylene glycol (both 2:1). This may be because, although the scintillation cocktail component absorbed by N910 accounts for the smallest proportion in the simulated waste liquid, it requires the lowest liquid-to-solid ratio, thus becoming the "short plank" factor of the absorption capacity of the entire mixed system and determining the overall optimal operating condition of the mixed absorbent.

4. Conclusions

In this study, aiming at the safe treatment of tritium containing measurement waste liquid, the absorption performance of commercial absorbents N910 and N960 toward each characteristic component in the waste liquid and toward the simulated tritium containing measurement waste liquid was systematically investigated. The main conclusions are as follows:

1. The absorption capacities of N910 for scintillation cocktail, and N960 for water and ethylene glycol, all increased with increasing liquid to solid ratio. However, excessively high liquid to solid ratios led to a significant increase in unabsorbed amounts, resulting in absorbent waste and additional burden for subsequent treatment. On the basis of comprehensive optimization, it was determined that the optimal liquid to solid ratio for N910 absorbing scintillation cocktail is 1.5:1, and the optimal liquid to solid ratios for N960 absorbing water and ethylene glycol are both 2:1.

2. The absorption capacities of N910 for scintillation cocktail and N960 for water both showed a continuous decreasing trend

with increasing temperature, while the absorption capacity of N960 for ethylene glycol varied only slightly within the experimental temperature range, remaining between 1.96 and 2.00 $g.g^{-1}$. Overall, all systems achieved relatively high absorption capacities under room temperature conditions, which is consistent with the ambient temperature conditions for the actual storage and treatment of tritium containing measurement waste liquid.

3. The absorption capacities of N910 for scintillation cocktail, and N960 for water and ethylene glycol, all exhibited typical characteristics of a rapid initial absorption stage followed by a subsequent slow equilibrium stage with increasing absorption time, and the equilibrium time was approximately 20 min for all systems. The equilibrium absorption capacities of N910 for scintillation cocktail, and N960 for water and ethylene glycol, were 1.48 $g.g^{-1}$, 1.99 $g.g^{-1}$, and 2.00 $g.g^{-1}$, respectively.

4. The pseudo second order kinetic equation could well describe the absorption processes of N910 for scintillation cocktail, and N960 for water and ethylene glycol. The linear correlation coefficients R2 were all close to unity, and the theoretical equilibrium absorption capacities were in excellent agreement with the experimental values. The results indicate that the above absorption processes are all dominated by chemisorption, and the underlying mechanisms are mainly the hydrophobic/π π interactions between the aromatic skeleton of N910 and scintillation cocktail molecules, as well as the hydrogen bonding between the polar functional groups (amide/amine groups) of N960 and water/ethylene glycol molecules.

On the basis of the optimal liquid to solid ratios for each component, the suitable mixing mass ratio of N960 to N910 was determined to be 5.25:1 through theoretical estimation. Under this ratio, the performance evaluation results of the mixed absorbent for the simulated tritium containing measurement waste liquid indicated that the optimal operating liquid to solid ratio is 1.5:1, at which the simulated waste liquid can be completely absorbed without free liquid residue. This mixed absorption scheme provides a feasible technical approach for the safe and efficient treatment of tritium containing measurement waste liquid.

References

1. Rahman ROA, Ibrahium HA, Hung YT (2011) Liquid Radioactive Wastes Treatment: A Review. Water 3: 551.

2. Chen L, Li J, Wang J (2024) Solidification of radioactive spent liquid scintillator wastes: Effect of additives on the compressive strength of the solidified forms. Nucl Eng Des 418: 112932.

3. Alok R, R N (2023) Treatment of laboratory generated radioactive organic liquid waste using a novel ionic liquid based resin: A feasibility study. J Mol Liq 390: 123079.

4. Lemont F, Marchand M, Mabrouk M, Milelli A, Baronnet JM (2017) ELIPSE: An Innovative Technology for the 5. Treatment of Radioactive Organic Liquids. Nucl Technol 198: 53-63.

5. Baranyi A, Kopecskó K (2022) Preliminarily Experiments of Liquid Scintillation Cocktail Waste Solidification. Period Polyt Civ Eng 66: 1234-1240.

6. Chunhai L, Yaxin H, Jiawei T, Liang M (2023) Safety of CDUT01 organic absorbent for radioactive organic liquid waste. J Radioanal Nucl Chem 332: 1015-1018.

7. Wang C, Yu G, Wang J (2024) Treatment of spent radioactive organic solvents from nuclear fuel reprocessing plant: Advances and perspectives. Nucl Eng Des 422: 113138.

8. Mabrouk M, Lemont F, Baronnet JM (2012) Incineration of radioactive organic liquid wastes by underwater thermal plasma. J Phys Conf Ser 406: 012002.

9. Mabrouk M, Marchand M, Baronnet JM, Lemont F (2016) Trichloroethylene combustion in a submerged thermal plasma: Results and chemical kinetics model. Plasma Chem Plasma Process 36: 1085-1110.

10. Barge AS, Vaidya PD (2018) Wet air oxidation of cresylic spent caustic – A model compound study over graphene oxide (GO) and ruthenium/GO catalysts. J Environ Manage 212: 479-489.

11. Mohite R, Garg A (2020) Performance of Supported Copper Catalysts for Oxidative Degradation of Phenolics in Aqueous Medium: Optimization of Reaction Conditions, Kinetics, Catalyst Stability, Characterization, and Reusability. Ind Eng Chem Res 59: 12986-12998.

12. Barbhuiya S, Das BB, Qureshi T, Adak D (2024) Cement-based solidification of nuclear waste: Mechanisms, formulations and regulatory considerations. J Environ Manage 356: 120712.

13. Chen L, Li J, Wang J (2024) Various additives for improving the performances of solidified forms of radioactive wastes by cementation technology: Recent advances and perspectives. Nucl Eng Des 429: 113595.

14. Mossini E, Santi A, Magugliani G, Galluccio F, Macerata E, et al. (2023) Pre-impregnation approach to encapsulate radioactive liquid organic waste in geopolymer. J Nucl Mater 585: 154608.

15. Liu J, Xu Y, Zhang W, Ye J, Wang R (2024) Solidification performance and mechanism of typical radioactive nuclear waste by geopolymers and geopolymer ceramics: A review. Prog Nucl Energy 169: 105106.

16. Charles R, Catherine D, Christel P, David L (2023) Trapping performance of alkali-activated materials incorporating a hy-

drogen/tritium getter for the conditioning of tritiated organic liquids. J Nucl Mater 576: 154272.

17. Xu Y, Kim SY, Ito T, Nakazawa K, Funaki Y, et al. (2012) Adsorption and separation behavior of yttrium and strontium in nitric acid solution by extraction chromatography using a macroporous silica-based adsorbent. J Chromatogr A 1263: 28-33.

18. Ahmed I, Lee G, Lee HJ, Jhung SH (2024) Adsorption of pharmaceuticals from water using metal-organic frameworks (MOFs), MOF-derived carbons, covalent-organic frameworks (COFs), COF-derived carbons: Comparison of the four adsorbents. Chem Eng J 488: 151022.

19. Nasser AH, Sahar S, P MA (2023) Three-Dimensional Printing of Cellulose/Covalent Organic Frameworks (CelloCOFs) for CO_2 Adsorption and Water Treatment. ACS Appl Mater Interfaces 15: 59795-59805.

20. Slava M, Viktor M (2023) Quantification of plastic shrinkage and plastic shrinkage cracking of the 3D printable concretes using 2D digital image correlation. Cem Concr Compos 139: 105050.

21. Cervantes-Uc JM, Cauich-Rodríguez JV, Herrera-Kao WA, Vázquez-Torres H, Marcos-Fernández A (2008) Thermal degradation behavior of polymethacrylates containing amine side groups. Polym Degrad Stab 93: 1891-1900.

22. Irene C, Daniele F, Andrea F, Cristian T, A SL, E SC (2023) Analytical pyrolysis of polyethyleneimines. J Anal Appl Pyrolysis 169: 105838.

23. Meng C, Liu X (2022) Study on thermal degradation kinetics of bio-based semi-aromatic high-temperature polyamide PA5T/56 and the effect of benzene ring. Iran Polym J 31: 1-10.

24. Zhu J, Deng C, Jiang H, Zheng Z, Gong R, et al. (2016) The impact of fluorescent dyes on the performances of polystyrene-based plastic scintillators. Nucl Instrum Methods Phys Res A 835: 136-141.

25. Xu Y, Deng H, Lei H, Chang G (2019) Initiator-free preparation and properties of polystyrene-based plastic scintillators. J Polym Res 26: 1-9.

26. Du X, Liu P, Qin GWZCWWH (2023) Comparative Study for Water Vapor Adsorption Thermodynamics in Different Clays. Energy Fuels 37: 13810-13828.

27. Hoffmann MM, Kealy JD, Gutmann T, Buntkowsky G (2022) Densities, Viscosities, and Self-Diffusion Coefficients of Several Polyethylene Glycols. J Chem Eng Data 67.